

## Adaptive Computation of the Corner Singularity with the Monotone Jump Condition Capturing Scheme

Yin-Liang Huang and Wei-Cheng Wang

ABSTRACT. We introduce a simple finite difference scheme for the elliptic interface problem. The scheme is symmetric, definite and monotone with second order accuracy. It is also quite naturally adapted to corner singularities. A simple adaptive strategy yields competitive performance even in the severe case of intersecting interfaces.

### 1. Introduction

In this report, we consider the elliptic interface problem

$$(1.1) \quad \nabla \cdot (\kappa(\mathbf{x})\nabla u(\mathbf{x})) = f(\mathbf{x}), \quad \mathbf{x} \in \Omega \setminus \Gamma,$$

where  $\kappa(\mathbf{x}) > 0$  is piecewise smooth but discontinuous across an interface  $\Gamma$ . Accompanied with the discontinuity of  $\kappa(\mathbf{x})$  are the following jump conditions prescribed along  $\Gamma$ :

$$(1.2) \quad \begin{aligned} [u]_{\Gamma} &= a(\mathbf{x}), & \mathbf{x} \in \Gamma, \\ [\kappa u_n]_{\Gamma} &= b(\mathbf{x}), & \mathbf{x} \in \Gamma. \end{aligned}$$

Here the jump  $[\cdot]$  denotes the difference between the limits from both sides of  $\Gamma$ .

The elliptic interface problem (1.1) arises naturally in many fields of science and engineering applications. Due to the presence of discontinuity in  $\kappa$ , standard numerical methods for continuous  $\kappa$  usually fail to reach optimal performance. There are many numerical methods specifically designed for (1.1), (1.2) with discontinuous  $\kappa$ .

When the interface  $\Gamma$  is smooth, the solution is piecewise smooth [8, 9, 11, 14]. In this case, local Taylor expansion is valid on either side of the interface  $\Gamma$ . In [12], LeVeque and Li devised a second order finite difference scheme on uniform Cartesian grids by matching the interface conditions (1.2) with local Taylor expansion to very high order. In contrast, Liu et al. [15] proposed a simple first order finite difference scheme also on uniform grids. The corresponding matrix is symmetric and definite and thus can be solved with standard iterative methods and preconditioning techniques. In [17], a different finite difference approach was

---

This work is supported in part by the National Science Committee of Taiwan under contract 93-2115-M-007-011.

proposed. Using a body-fitting curvilinear coordinate system and the covariant form of (1.1) together with an unusual choice of computational variables, a second order centered difference scheme was constructed. The interface conditions (1.2) are incorporated into the discretization and the corresponding stiffness matrix is symmetric, definite and very easy to generate. Both the numerical solution and the flux are observed to have second order accuracy.

There are also finite element methods designed specifically for (1.1) and (1.2). In [1, 2, 5] the elements are constructed by matching element edges with the interface  $\Gamma$ . Various treatments have been proposed to handle the interface conditions in [1, 2, 5] and an optimal error estimate in the energy norm was given in [5] for standard linear finite elements. An alternative treatment was proposed by Li et al. [13]. There the special basis functions satisfying the interface conditions (1.2) were constructed to span the finite element space, thus no need to enforce them explicitly in the Galerkin approximation.

When the interface contains a corner or crosses itself, the solution is potentially singular [10]. In this case, local mesh refinement near the corner is necessary to obtain reasonable accuracy. It is shown in [16] and [4] that if the error estimator is properly chosen, one can efficiently distribute the grids and get near optimal performance.

In the special case where the interface are straight lines and  $f$  is locally self-similar, Han [6] and Yin [18] proposed an infinite element method for singular elliptic interface problems. Utilizing the self-similarity of the solution and the elements, the infinite stiffness matrix can be generated by a transition matrix which acts on neighboring layers of nested elements. Thus the computational cost is effectively reduced. However, this method does not seem to be applicable to curved interfaces.

In this paper, we report an improved version of the jump condition capturing scheme described in [17]. With elaborations on mixing discretizations from different coordinate directions, the corresponding matrix is constructed with built-in symmetry, definiteness and monotonicity (M-matrix). Moreover, we find the scheme quite natural for corner singularities. With a deformed local polar coordinate system and an adaptive stretching of the radial variable, our scheme is capable of resolving the corner singularity to satisfaction. The adaptive procedure is very simple and the result is comparable to those obtained by adaptive mesh refinement based on *a posteriori* error estimates proposed in [5, 16].

The rest of this paper is organized as follows. In section 2, we describe the covariant form of the elliptic interface problem in general curvilinear coordinate systems and the numerical discretization of the metric tensors in the standard coordinate and the “skewed” coordinate. In section 3, we introduce a symmetry preserving averaging procedure that mixes the two different schemes from two sets of coordinates. We also obtain a sufficient condition on grid skewness such that a monotone discretization of (1.1) can be so obtained. In section 4, we show how to incorporate the interface conditions (1.2) into the monotone discretization and finally in section 5, we report the numerical result of a singular problem with self-crossing interfaces using our scheme.

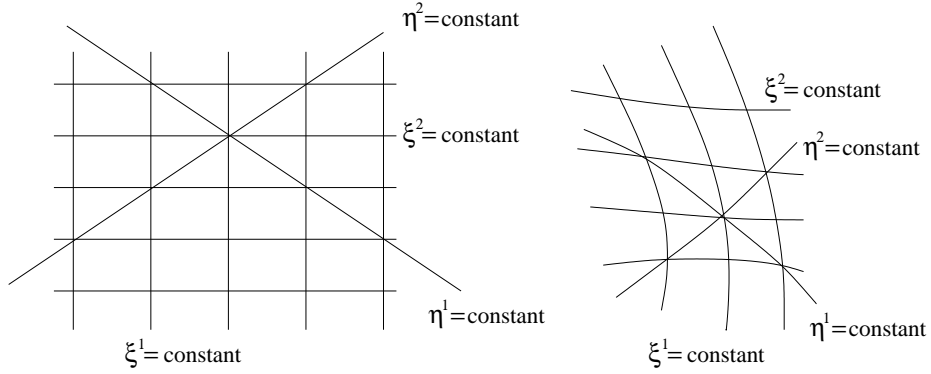


**Figure 1:** The curvilinear coordinate and the skewed coordinate.

## 2. Curvilinear Coordinate and Metric Tensors

For simplicity of presentation, we first assume that a physical domain  $\mathcal{R}$  can be mapped smoothly from a rectangular computational domain with  $\kappa$  and the exact solution to (1.1) being smooth in  $\mathcal{R}$ . The general case is described in Section 4.

In a general curvilinear coordinate system, (1.1) can be written as:

$$(2.1) \quad \nabla \cdot (\kappa \nabla u) = \frac{1}{\sqrt{g}} \partial_\alpha (\kappa \sqrt{g} g^{\alpha\beta} \partial_\beta u) = f$$

or the symmetrized form:

$$(2.2) \quad \partial_\alpha (\kappa \sqrt{g} g^{\alpha\beta} \partial_\beta u) = \sqrt{g} f$$

where summation convention is adopted and  $\partial_\alpha$  denotes the partial derivative with respect to  $\xi^\alpha$ . The metric tensors in (2.2) are defined by

$$(2.3) \quad g^{\alpha\beta} := \langle \nabla \xi^\alpha, \nabla \xi^\beta \rangle,$$

$$(2.4) \quad g_{\alpha\beta} := \left\langle \frac{\partial \mathbf{x}}{\partial \xi^\alpha}, \frac{\partial \mathbf{x}}{\partial \xi^\beta} \right\rangle,$$

$$(2.5) \quad g := \det(g_{\alpha\beta}),$$

$$(2.6) \quad \sqrt{g} = \det \left( \frac{\partial \mathbf{x}}{\partial \xi} \right),$$

$$(2.7) \quad g^{\alpha\lambda} g_{\lambda\beta} = \delta_\beta^\alpha.$$

Equation (2.2) is valid in any coordinate system. Instead of discretizing (2.2) in the  $\xi$  variables directly, it turns out to be easier to construct a symmetric and definite discretization for (1.1) in the skewed direction [17]. In other words, we define

$$(2.8) \quad \eta^1 := \frac{\xi^1 h_2 + \xi^2 h_1}{\ell}, \quad \eta^2 := \frac{\xi^2 h_1 - \xi^1 h_2}{\ell}$$

where  $\ell := \sqrt{h_1^2 + h_2^2}$ , and

$$h := \Delta\eta^1 = \Delta\eta^2 = \frac{2h_1h_2}{\ell}.$$

The interface problem (1.1) can be written in the  $\eta$  coordinates as

$$(2.9) \quad \widehat{\partial}_\mu(\kappa\sqrt{\widehat{g}}\widehat{g}^{\mu\nu}\widehat{\partial}_\nu u) = \sqrt{\widehat{g}}f$$

where  $\widehat{\partial}_\mu$  is the partial derivative with respect to  $\eta^\mu$  and  $\widehat{g}^{\mu\nu}$ ,  $\widehat{g}_{\mu\nu}$ , and  $\widehat{g}$  are defined as (2.3)-(2.7) with  $\xi^\alpha$  replaced by  $\eta^\mu$ .

A second order approximation of the metric tensors for the  $\eta$  variables can be conveniently computed from  $\mathbf{x}_{i,j}$  via centered difference:

$$\begin{aligned} ((\widehat{g}_{11})_h)_{i+\frac{1}{2},j+\frac{1}{2}} &:= \left\langle \frac{\mathbf{x}_{i+1,j+1} - \mathbf{x}_{i,j}}{h}, \frac{\mathbf{x}_{i+1,j+1} - \mathbf{x}_{i,j}}{h} \right\rangle, \\ ((\widehat{g}_{22})_h)_{i+\frac{1}{2},j+\frac{1}{2}} &:= \left\langle \frac{\mathbf{x}_{i,j+1} - \mathbf{x}_{i+1,j}}{h}, \frac{\mathbf{x}_{i,j+1} - \mathbf{x}_{i+1,j}}{h} \right\rangle, \\ ((\widehat{g}_{12})_h)_{i+\frac{1}{2},j+\frac{1}{2}} = ((\widehat{g}_{21})_h)_{i+\frac{1}{2},j+\frac{1}{2}} &:= \left\langle \frac{\mathbf{x}_{i+1,j+1} - \mathbf{x}_{i,j}}{h}, \frac{\mathbf{x}_{i,j+1} - \mathbf{x}_{i+1,j}}{h} \right\rangle, \\ \widehat{g}_h^{\mu\lambda}(\widehat{g}_{\lambda\nu})_h &= \delta_\nu^\mu. \end{aligned}$$

The discretization of (2.9) is then given by

$$(2.10) \quad (\widehat{\mathbf{L}}(\kappa)u)_{i,j} := \widehat{\mathcal{D}}_\mu(\kappa\sqrt{\widehat{g}_h}\widehat{g}_h^{\mu\nu}\widehat{\mathcal{D}}_\nu u)_{i,j},$$

where

$$(\widehat{\mathcal{D}}_1 u)_{i,j} = \frac{u_{i+\frac{1}{2},j+\frac{1}{2}} - u_{i-\frac{1}{2},j-\frac{1}{2}}}{h}, \quad (\widehat{\mathcal{D}}_2 u)_{i,j} = \frac{u_{i-\frac{1}{2},j+\frac{1}{2}} - u_{i+\frac{1}{2},j-\frac{1}{2}}}{h},$$

and the indices  $(i,j)$  refer to the  $\xi$  variables, not  $\eta$ .

Since

$$(2.11) \quad \sum_i \psi_i(\mathcal{D}\phi)_i = - \sum_i (\mathcal{D}\psi)_{i-\frac{1}{2}}\phi_{i-\frac{1}{2}},$$

we have

$$(2.12) \quad \begin{aligned} \sum_{i,j} \psi_{i,j}(\widehat{\mathbf{L}}\phi)_{i,j} &= \sum_{i,j} \psi_{i,j}\widehat{\mathcal{D}}_\mu(\kappa\sqrt{\widehat{g}_h}\widehat{g}_h^{\mu\nu}\widehat{\mathcal{D}}_\nu\phi)_{i,j} \\ &= - \sum_{i,j} \kappa\sqrt{\widehat{g}_h}\widehat{g}_h^{\mu\nu}(\widehat{\mathcal{D}}_\mu\psi)(\widehat{\mathcal{D}}_\nu\phi)_{i+\frac{1}{2},j+\frac{1}{2}} = \sum_{i,j} (\widehat{\mathbf{L}}\psi)_{i,j}\phi_{i,j} \end{aligned}$$

and

$$(2.13) \quad \begin{aligned} - \sum_{i,j} \phi_{i,j}(\widehat{\mathbf{L}}\phi)_{i,j} &= - \sum_{i,j} \phi_{i,j}\widehat{\mathcal{D}}_\mu(\kappa\sqrt{\widehat{g}_h}\widehat{g}_h^{\mu\nu}\widehat{\mathcal{D}}_\nu\phi)_{i,j} \\ &= \sum_{i,j} \kappa\sqrt{\widehat{g}_h}\widehat{g}_h^{\mu\nu}(\widehat{\mathcal{D}}_\mu\phi)(\widehat{\mathcal{D}}_\nu\phi)_{i+\frac{1}{2},j+\frac{1}{2}} \geq 0. \end{aligned}$$

where for simplicity of presentation, we have ignored the boundary terms in (2.11), (2.12) and (2.13). It follows that  $\widehat{\mathbf{L}}(\kappa)$  is symmetric and (non-positive) definite.

The discretization of (2.2) in the  $\xi^\alpha$  variables is more complicated. It is given by [7]

$$\mathbf{L}(\kappa) = \mathbf{L}_{11}(\kappa) + \mathbf{L}_{21}(\kappa) + \mathbf{L}_{12}(\kappa) + \mathbf{L}_{22}(\kappa),$$

where

$$\begin{aligned}
(\mathbf{L}_{11}(\kappa)u)_{i,j} &:= \left( \mathcal{D}_1(\mathcal{A}_2(\kappa\sqrt{g_h}g_h^{11})\mathcal{D}_1u) \right)_{i,j} \\
(\mathbf{L}_{12}(\kappa)u)_{i,j} &:= \left( \mathcal{D}_1\mathcal{A}_2(\kappa\sqrt{g_h}g_h^{12})\mathcal{A}_1\mathcal{D}_2u \right)_{i,j} \\
(\mathbf{L}_{21}(\kappa)u)_{i,j} &:= \left( \mathcal{D}_2\mathcal{A}_1(\kappa\sqrt{g_h}g_h^{21})\mathcal{A}_2\mathcal{D}_1u \right)_{i,j} \\
(\mathbf{L}_{22}(\kappa)u)_{i,j} &:= \left( \mathcal{D}_2(\mathcal{A}_1(\kappa\sqrt{g_h}g_h^{22})\mathcal{D}_2u) \right)_{i,j}
\end{aligned}
\tag{2.14}$$

with

$$(\mathcal{D}_1u)_{i,j} := \frac{u_{i+\frac{1}{2},j} - u_{i-\frac{1}{2},j}}{h_1}, \quad (\mathcal{D}_2u)_{i,j} := \frac{u_{i,j+\frac{1}{2}} - u_{i,j-\frac{1}{2}}}{h_2},$$

and

$$(\mathcal{A}_1u)_{i,j} := \frac{u_{i+\frac{1}{2},j} + u_{i-\frac{1}{2},j}}{2}, \quad (\mathcal{A}_2u)_{i,j} := \frac{u_{i,j+\frac{1}{2}} + u_{i,j-\frac{1}{2}}}{2}.$$

In (2.14), we find it convenient to evaluate the numerical metric tensors by way of

$$\begin{aligned}
(g_h^{11})_{i+\frac{1}{2},j+\frac{1}{2}} &:= \frac{\ell^2}{4h_2^2} (\widehat{g}_h^{11} + \widehat{g}_h^{22} - 2\widehat{g}_h^{12})_{i+\frac{1}{2},j+\frac{1}{2}}, \\
(g_h^{22})_{i+\frac{1}{2},j+\frac{1}{2}} &:= \frac{\ell^2}{4h_1^2} (\widehat{g}_h^{11} + \widehat{g}_h^{22} + 2\widehat{g}_h^{12})_{i+\frac{1}{2},j+\frac{1}{2}}, \\
(g_h^{12})_{i+\frac{1}{2},j+\frac{1}{2}} &= (g_h^{21})_{i+\frac{1}{2},j+\frac{1}{2}} := \frac{\ell^2}{4h_1h_2} (\widehat{g}_h^{11} - \widehat{g}_h^{22})_{i+\frac{1}{2},j+\frac{1}{2}} \\
&\quad \sqrt{g_h} := m^{-1}\sqrt{\widehat{g}_h} \quad \text{where } m := (2h_1h_2)^{-1}\ell^2.
\end{aligned}
\tag{2.15}$$

The continuum analogue of (2.15) can be derived easily from (2.3)-(2.6) and (2.8).

The discretization (2.14) is deliberately constructed with built-in symmetry and non-positivity. Indeed, from (2.11) and the following identity

$$(2.16) \quad \sum_i \psi_i(\mathcal{A}\phi)_i = \sum_i (\mathcal{A}\psi)_{i-\frac{1}{2}}\phi_{i-\frac{1}{2}}$$

we can derive

$$\begin{aligned}
& - \sum \phi_{i,j} (\mathbf{L}(\kappa)\phi)_{i,j} \\
&= - \sum \phi_{i,j} \left( \mathcal{D}_1(\mathcal{A}_2(\kappa\sqrt{g_h}g_h^{11})\mathcal{D}_1\phi) \right)_{i,j} - \sum \phi_{i,j} \left( \mathcal{D}_2(\mathcal{A}_1(\kappa\sqrt{g_h}g_h^{22})\mathcal{D}_2\phi) \right)_{i,j} \\
&\quad - \sum \phi_{i,j} \left( \mathcal{D}_2\mathcal{A}_1(\kappa\sqrt{g_h}g_h^{21})\mathcal{A}_2\mathcal{D}_1\phi \right)_{i,j} - \sum \phi_{i,j} \left( \mathcal{D}_1\mathcal{A}_2(\kappa\sqrt{g_h}g_h^{12})\mathcal{A}_1\mathcal{D}_2\phi \right)_{i,j} \\
&= \sum \left( \mathcal{A}_2(\kappa\sqrt{g_h}g_h^{11})(\mathcal{D}_1\phi)^2 \right)_{i+\frac{1}{2},j} + \sum \left( \mathcal{A}_1(\kappa\sqrt{g_h}g_h^{22})(\mathcal{D}_2\phi)^2 \right)_{i,j+\frac{1}{2}} \\
&\quad + 2 \sum \left( \kappa\sqrt{g_h}g_h^{12}(\mathcal{A}_1\mathcal{D}_2\phi)(\mathcal{A}_2\mathcal{D}_1\phi) \right)_{i+\frac{1}{2},j+\frac{1}{2}},
\end{aligned}
\tag{2.17}$$

where for simplicity, we have again ignored boundary terms in (2.16)-(2.17). Moreover,

$$\begin{aligned}
(2.18) \quad & 2 \left| \sum \left( \kappa \sqrt{g_h} g_h^{12} (\mathcal{A}_1 \mathcal{D}_2 \phi) (\mathcal{A}_2 \mathcal{D}_1 \phi) \right)_{i+\frac{1}{2}, j+\frac{1}{2}} \right| \\
& \leq \sum \left( \kappa \sqrt{g_h} g_h^{11} (\mathcal{A}_2 \mathcal{D}_1 \phi) \right)_{i+\frac{1}{2}, j+\frac{1}{2}}^2 + \sum \left( \kappa \sqrt{g_h} g_h^{22} (\mathcal{A}_1 \mathcal{D}_2 \phi) \right)_{i+\frac{1}{2}, j+\frac{1}{2}}^2 \\
& \leq \sum \left( \kappa \sqrt{g_h} g_h^{11} \mathcal{A}_2 (\mathcal{D}_1 \phi)^2 \right)_{i+\frac{1}{2}, j+\frac{1}{2}} + \sum \left( \kappa \sqrt{g_h} g_h^{22} \mathcal{A}_1 (\mathcal{D}_2 \phi)^2 \right)_{i+\frac{1}{2}, j+\frac{1}{2}} \\
& = \sum \left( \mathcal{A}_2 (\kappa \sqrt{g_h} g_h^{11}) (\mathcal{D}_1 \phi)^2 \right)_{i+\frac{1}{2}, j} + \sum \left( \mathcal{A}_1 (\kappa \sqrt{g_h} g_h^{22}) (\mathcal{D}_2 \phi)^2 \right)_{i, j+\frac{1}{2}}.
\end{aligned}$$

therefore we conclude that

$$- \sum \phi_{i,j} (\mathbf{L}(\kappa) \phi)_{i,j} \geq 0,$$

A similar calculation as in (2.12) also leads to

$$\sum_{i,j} \psi_{i,j} (\mathbf{L}(\kappa) \phi)_{i,j} = \sum_{i,j} (\mathbf{L}(\kappa) \psi)_{i,j} \phi_{i,j}.$$

Thus  $\mathbf{L}(\kappa)$  is symmetric and definite.

### 3. Symmetry Preserving Average and Monotonicity

Both  $\widehat{\mathbf{L}}$  and  $\mathbf{L}$  are of the form

$$\sum_{k=i-1}^{i+1} \sum_{l=j-1}^{j+1} a_{k,l} u_{k,l} \quad \text{with} \quad \sum_{k=i-1}^{i+1} \sum_{l=j-1}^{j+1} a_{k,l} = 0.$$

Such an operator is monotone provided  $a_{i,j} < 0$  and  $a_{k,l} \geq 0$  for  $(k,l) \neq (i,j)$ . It is easy to see that neither  $\widehat{\mathbf{L}}$  nor  $\mathbf{L}$  is monotone. However, each has a favored direction in which the coefficients has the preferred sign. Motivated by this, we define the following symmetrically averaged operator with an auxiliary weight function  $w$  defined on the cell centers as free parameters:

(3.1)

$$\begin{aligned}
\mathbf{M}u & := \widehat{\mathbf{L}}(w\kappa)u + m\mathbf{L}((1-w)\kappa)u \\
& = \widehat{\mathcal{D}}_\mu(w\kappa \sqrt{\widehat{g}_h} \widehat{g}_h^{\mu\nu} \widehat{\mathcal{D}}_\nu u) \\
& \quad + m\mathcal{D}_1 (\mathcal{A}_2 ((1-w)\kappa \sqrt{g_h} g_h^{11}) \mathcal{D}_1 u) + m\mathcal{D}_2 (\mathcal{A}_1 ((1-w)\kappa \sqrt{g_h} g_h^{22}) \mathcal{D}_2 u) \\
& \quad + m\mathcal{D}_2 \mathcal{A}_1 ((1-w)\kappa \sqrt{g_h} g_h^{21}) \mathcal{A}_2 \mathcal{D}_1 u + m\mathcal{D}_1 \mathcal{A}_2 ((1-w)\kappa \sqrt{g_h} g_h^{12}) \mathcal{A}_1 \mathcal{D}_2 u.
\end{aligned}$$

It follows that if  $u^e$  is the exact solution of (1.1) and  $w$  sufficiently smooth, we have

$$\begin{aligned}
(3.2) \quad & \widehat{\mathbf{L}}(w\kappa)u^e + m\mathbf{L}((1-w)\kappa)u^e \\
& = \sqrt{\widehat{g}} \nabla \cdot (w\kappa \nabla u^e) + m\sqrt{g} \nabla \cdot ((1-w)\kappa \nabla u^e) + O(h^2) \\
& = \sqrt{\widehat{g}} (w + (1-w)) \nabla \cdot (\kappa \nabla u^e) + \sqrt{\widehat{g}} (\nabla w + \nabla(1-w)) \cdot \kappa \nabla u^e + O(h^2) \\
& = \sqrt{\widehat{g}} f + O(h^2).
\end{aligned}$$

Therefore  $\mathbf{M}$  is consistent with  $\sqrt{\widehat{g}_h} \nabla \cdot (\kappa \nabla u)$  to second order. One can also show similarly that  $w\widehat{\mathbf{L}}(\kappa)u^e + (1-w)m\mathbf{L}(\kappa)u^e = \sqrt{\widehat{g}} f + O(h^2)$ . However, the operator

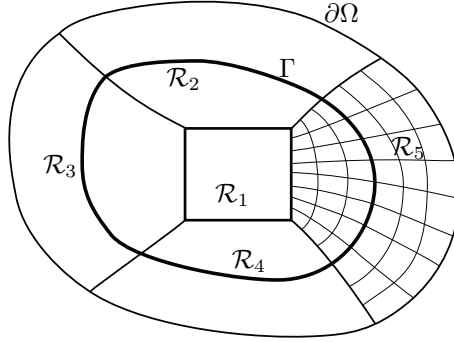


**Figure 2:** non-overlapping quadrilateral decomposition of  $\Omega$ .

$w\widehat{\mathbf{L}}(\kappa) + (1-w)m\mathbf{L}(\kappa)$  is no longer symmetric for non-constant weight functions  $w$ .

For the symmetrically averaged operator  $\mathbf{M}$ , we have the following equivalent condition for monotonicity of  $\mathbf{M}$  [7]:

**THEOREM 1.** *Define*

$$(3.3) \quad \tilde{g}_h^{11} = \frac{h_2}{h_1} g_h^{11}, \quad \tilde{g}_h^{22} = \frac{h_1}{h_2} g_h^{22} \quad \text{and} \quad \tilde{g}_h^{12} = g_h^{12}.$$

Then there exists a weight function  $w$  with  $0 \leq w \leq 1$  such that  $\mathbf{M}$  is monotone if

$$(3.4) \quad \left| (\tilde{g}_h^{12})_{i+\frac{1}{2}, j+\frac{1}{2}} \right| \leq \min \left\{ (\tilde{g}_h^{11})_{i+\frac{1}{2}, j+\frac{1}{2}}, (\tilde{g}_h^{22})_{i+\frac{1}{2}, j+\frac{1}{2}} \right\}$$

for all  $i, j$ .

When (3.4) holds, a symmetric, definite and monotone discretization of (2.2) is thus given by

$$(3.5) \quad \mathbf{M}u = \sqrt{\widehat{g}_h} f$$

with the corresponding weight function  $w$ .

#### 4. Capturing the Jump Conditions on the Interface

For general domains with  $\kappa$  discontinuous across an interface  $\Gamma$ , we can decompose the domain into non-overlapping quadrilateral sub-domains with the material interface  $\Gamma$  aligned with coordinate lines. An example is given in figure 2. When  $\Gamma$  is smooth and not self-crossing, we may assume, without loss of generality, that  $\kappa$  and  $g^{\alpha\beta}$  are piecewise smooth and may be discontinuous across the material interface  $\Gamma$  and/or coordinate interfaces. Since all the derivatives are approximated by centered differences, the local truncation error is therefore  $O(h^2)$  within each sub-domain except on  $\Gamma$ .

We now proceed to show that (3.5) can be generalized to material/coordinate interfaces. The symmetry, non-positivity and monotonicity remain and the local truncation error is  $O(h)$  on the interfaces. Suppose the interface is aligned with a coordinate surface  $\xi^1 = \text{constant}$ , or  $i = i_0$ . For simplicity of presentation, we assume  $[u] = 0$  across  $\Gamma$ . The general case can be similarly derived with slight

modification. We collect the ‘‘right’’ part of  $\mathbf{L}$ , which are terms in  $\mathbf{L}$  involving the quantities defined on  $(i + \frac{1}{2}, j + \frac{1}{2})$  and  $(i + \frac{1}{2}, j - \frac{1}{2})$  and name the corresponding portion  $\mathbf{L}_R(\kappa)$ . In other words,

$$(\mathbf{L}_R(\kappa)u)_{i,j} = (A) + (B) + (C)$$

where

$$(A) := (\kappa\sqrt{g_h}g_h^{12})_{i+\frac{1}{2},j+\frac{1}{2}} \left( \frac{u_{i+1,j+1} - u_{i,j}}{2h_1h_2} \right) + (\kappa\sqrt{g_h}g_h^{12})_{i+\frac{1}{2},j-\frac{1}{2}} \left( \frac{u_{i,j} - u_{i+1,j-1}}{2h_1h_2} \right),$$

$$(B) := \frac{1}{2h_1} \left( (\kappa\sqrt{g_h}g_h^{11})_{i+\frac{1}{2},j+\frac{1}{2}} + (\kappa\sqrt{g_h}g_h^{11})_{i+\frac{1}{2},j-\frac{1}{2}} \right) \left( \frac{u_{i+1,j} - u_{i,j}}{h_1} \right),$$

$$(C) := (\kappa\sqrt{g_h}g_h^{22})_{i+\frac{1}{2},j+\frac{1}{2}} \left( \frac{u_{i,j+1} - u_{i,j}}{2(h_2)^2} \right) - (\kappa\sqrt{g_h}g_h^{22})_{i+\frac{1}{2},j-\frac{1}{2}} \left( \frac{u_{i,j} - u_{i,j-1}}{2(h_2)^2} \right).$$

For a piecewise smooth function  $u$ , (A)-(C) can be written as

$$(A) = \frac{h}{2h_1h_2} (\kappa\sqrt{g}g^{12}\widehat{\partial}_1u)_{i+\frac{1}{2},j+\frac{1}{2}} + \frac{h}{2h_1h_2} (\kappa\sqrt{g}g^{12}\widehat{\partial}_2u)_{i+\frac{1}{2},j-\frac{1}{2}} + O(h),$$

$$(B) = \frac{1}{h_1} (\kappa\sqrt{g}g^{11}\partial_1u)_{i+\frac{1}{2},j} + O(h),$$

$$(C) = \frac{1}{2h_2} \left( \left( \kappa\sqrt{g}g^{22} + \frac{h_1}{2}\partial_1(\kappa\sqrt{g}g^{22}) \right) \partial_2u \right)_{i^+,j+\frac{1}{2}} - \frac{1}{2h_2} \left( \left( \kappa\sqrt{g}g^{22} + \frac{h_1}{2}\partial_1(\kappa\sqrt{g}g^{22}) \right) \partial_2u \right)_{i^+,j-\frac{1}{2}} + O(h).$$

Since

$$\widehat{\partial}_1u = \frac{\ell}{2h_2}\partial_1u + \frac{\ell}{2h_1}\partial_2u \quad \text{and} \quad \widehat{\partial}_2u = \frac{-\ell}{2h_2}\partial_1u + \frac{\ell}{2h_1}\partial_2u,$$

we have

$$(A) = \frac{h}{2h_1h_2} \left( (\kappa\sqrt{g}g^{12}) \partial_1u \cdot \frac{\ell}{2h_2} + (\kappa\sqrt{g}g^{12}) \partial_2u \cdot \frac{\ell}{2h_1} \right)_{i+\frac{1}{2},j+\frac{1}{2}} + \frac{h}{2h_1h_2} \left( -(\kappa\sqrt{g}g^{12}) \partial_1u \cdot \frac{\ell}{2h_2} + (\kappa\sqrt{g}g^{12}) \partial_2u \cdot \frac{\ell}{2h_1} \right)_{i+\frac{1}{2},j-\frac{1}{2}} + O(h).$$

Next we expand these terms around  $(i + \frac{1}{2}, j)$  and combine (A) with (B) to get

$$\begin{aligned} (A) + (B) &= \frac{1}{2}\partial_2(\kappa\sqrt{g}g^{12}\partial_1u)_{i+\frac{1}{2},j} + \frac{1}{h_1}(\kappa\sqrt{g}g^{12}\partial_2u)_{i+\frac{1}{2},j} \\ &\quad + \frac{1}{h_1}(\kappa\sqrt{g}g^{11}\partial_1u)_{i+\frac{1}{2},j} + O(h) \\ &= \frac{1}{2}\partial_2(\kappa\sqrt{g}g^{12}\partial_1u)_{i^+,j} + \frac{1}{h_1}(\kappa\sqrt{g}g^{12}\partial_2u)_{i^+,j} + \frac{1}{2}\partial_1(\kappa\sqrt{g}g^{12}\partial_2u)_{i^+,j} \\ &\quad + \frac{1}{h_1}(\kappa\sqrt{g}g^{11}\partial_1u)_{i^+,j} + \frac{1}{2}\partial_1(\kappa\sqrt{g}g^{11}\partial_1u)_{i^+,j} + O(h). \end{aligned}$$

Expanding (C) around  $(i^+, j)$  gives

$$\begin{aligned} \text{(C)} &= \frac{1}{2h_2} \left( \left( \kappa\sqrt{g}g^{22} + \frac{h_1}{2}\partial_1(\kappa\sqrt{g}g^{22}) \right) \partial_2 u \right)_{i^+, j+\frac{1}{2}} \\ &\quad - \frac{1}{2h_2} \left( \left( \kappa\sqrt{g}g^{22} + \frac{h_1}{2}\partial_1(\kappa\sqrt{g}g^{22}) \right) \partial_2 u \right)_{i^+, j-\frac{1}{2}} + O(h) \\ &= \frac{1}{2}\partial_2(\kappa\sqrt{g}g^{22}\partial_2 u)_{i^+, j} + O(h). \end{aligned}$$

If  $u^e$  is the exact solution of (2.2),

$$(4.1) \quad (\mathbf{L}_R(\kappa)u^e)_{i,j} = \left( \frac{|\nabla\xi^1|\sqrt{g}}{h_1}(\kappa u_n^e) \right)_{i^+, j} + \frac{(\sqrt{g}f)_{i^+, j}}{2} + O(h).$$

Moreover,

$$|\nabla\xi^1|\sqrt{g} = \sqrt{g^{11}} \cdot \sqrt{g} = \sqrt{\frac{g_{22}}{g}} \cdot \sqrt{g} = \sqrt{g_{22}}$$

is continuous across the interface, therefore

$$(4.2) \quad (\mathbf{L}_R(\kappa)u^e)_{i,j} = \left( \frac{\sqrt{g_{22}}}{h_1}(\kappa u_n^e) \right)_{i^+, j} + \frac{(\sqrt{g}f)_{i^+, j}}{2} + O(h).$$

Similarly, we can define  $\mathbf{L}_L(\kappa)$  and conclude that

$$(4.3) \quad (\mathbf{L}_L(\kappa)u^e)_{i,j} = \left( \frac{-\sqrt{g_{22}}}{h_1}(\kappa u_n^e) \right)_{i^-, j} + \frac{(\sqrt{g}f)_{i^-, j}}{2} + O(h).$$

Therefore

$$\begin{aligned} (\mathbf{L}(\kappa)u^e)_{i,j} &= (\mathbf{L}_L(\kappa)u^e)_{i,j} + (\mathbf{L}_R(\kappa)u^e)_{i,j} \\ &= \left( \frac{\sqrt{g_{22}}}{h_1}[\kappa u_n^e] \right)_{i,j} + \frac{(\sqrt{g}f)_{i^+, j} + (\sqrt{g}f)_{i^-, j}}{2} + O(h) \end{aligned}$$

on  $\Gamma$ . On a coordinate interface, we simply replace  $[\kappa u_n^e]$  by 0. Similarly, we have

$$(\widehat{\mathbf{L}}(\kappa)u^e)_{i,j} = \left( \frac{m\sqrt{g_{22}}}{h_1}[\kappa u_n^e] \right)_{i,j} + \frac{(\sqrt{\widehat{g}}f)_{i^+, j} + (\sqrt{\widehat{g}}f)_{i^-, j}}{2} + O(h)$$

on the interface. Using a similar argument as in (3.2), we can derive

$$\begin{aligned} (\mathbf{M}(\kappa)u^e)_{i,j} &= \widehat{\mathbf{L}}(w\kappa)(u) + m\mathbf{L}((1-w)\kappa)(u) \\ &= \left( \frac{m\sqrt{g_{22}}}{h_1}[\kappa u_n^e] \right)_{i,j} + \frac{(\sqrt{\widehat{g}}f)_{i^+, j} + (\sqrt{\widehat{g}}f)_{i^-, j}}{2} + O(h) \end{aligned}$$

on the interface. Overall the monotone jump condition capturing scheme is given by

$$(4.4) \quad (\mathbf{M}(\kappa)u)_{i,j} = \begin{cases} \left( \frac{m\sqrt{(g_{22})_h}}{h_1}[\kappa u_n] \right)_{i,j} + \frac{(\sqrt{\widehat{g}_h}f)_{i^+, j} + (\sqrt{\widehat{g}_h}f)_{i^-, j}}{2} & (i, j) \text{ on an interface,} \\ (\sqrt{\widehat{g}_h}f)_{i,j} & \text{otherwise.} \end{cases}$$

Thus  $\mathbf{M}$  is monotone with local truncation error  $O(h)$  on the interface and  $O(h^2)$  elsewhere. From the classical pointwise estimate of discrete Green's function [3] and the discrete maximum principle, we have the following error estimate:

**COROLLARY 1.** *If the exact solution  $u^e$  is piecewise smooth on each region separated by  $\Gamma$ , then*

$$|u^e - u^h|_{i,j} \leq Ch^2 \log h.$$

We remark here that (4.2)-(4.3) and the corresponding counter part for  $\widehat{\mathbf{L}}$  can be used to reconstruct the numerical flux:

$$(4.5) \quad (\kappa u_n^h)_{i^+,j} := \frac{h_1}{m(\sqrt{(g_{22})_h})_{i,j}} \left( (\mathbf{M}_R u^h)_{i,j} - \frac{(\sqrt{g_h} f)_{i^+,j}}{2} \right)$$

and

$$(4.6) \quad (\kappa u_n^h)_{i^-,j} := \frac{-h_1}{m(\sqrt{(g_{22})_h})_{i,j}} \left( (\mathbf{M}_L u^h)_{i,j} - \frac{(\sqrt{g_h} f)_{i^-,j}}{2} \right).$$

The reconstructed numerical flux satisfies the interface condition *exactly*:

$$[\kappa u_n^h]_{i,j} = \frac{h_1}{m(\sqrt{(g_{22})_h})_{i,j}} \left( (\mathbf{M} u^h)_{i,j} - \frac{(\sqrt{g_h} f)_{i^+,j} + (\sqrt{g_h} f)_{i^-,j}}{2} \right) = [\kappa u_n]_{i,j}.$$

We have done extensive numerical simulations and observed that for piecewise smooth solutions, the reconstructed numerical flux is pointwise second order accurate [7].

## 5. Resolving the Point Singularity

When the interface contains a corner or is self-intersecting, the solution may develop singularity. Following is a well known example where the exact solution is barely in  $H^1$  [10]. In this example, the interface is given by  $\theta = 0, \pi/2, \pi$  and  $3\pi/2$  in the polar coordinate. The diffusion coefficient is piecewise constant. It takes the value  $\kappa^+$  in the first and third quadrants, and  $\kappa^- = 1$  in the second and fourth quadrants.

An exact solution of (1.1) with

$$(5.1) \quad f = 0, \quad [u] = [\kappa u_n] = 0$$

is given by  $v_1(r, \theta) = r^\gamma v(\theta)$ , where

$$v(\theta) = \begin{cases} \cos((\pi/2 - \sigma)\gamma) \cdot \cos((\theta - \pi/2 + \tau)\gamma) & \text{if } 0 \leq \theta \leq \pi/2, \\ \cos(\tau\gamma) \cdot \cos((\theta - \pi + \sigma)\gamma) & \text{if } \pi/2 \leq \theta \leq \pi, \\ \cos(\sigma\gamma) \cdot \cos((\theta - \pi - \tau)\gamma) & \text{if } \pi \leq \theta \leq 3\pi/2, \\ \cos((\pi/2 - \tau)\gamma) \cdot \cos((\theta - 3\pi/2 - \sigma)\gamma) & \text{if } 3\pi/2 \leq \theta \leq 2\pi, \end{cases}$$

and the parameters  $\gamma$ ,  $\tau$ ,  $\sigma$ ,  $\kappa^+$  are related to each other through the following relations

$$(5.2) \quad \begin{cases} \kappa^+ = -\tan((\pi/2 - \sigma)\gamma) \cdot \cot(\tau\gamma), \\ 1/\kappa^+ = -\tan(\tau\gamma) \cdot \cot(\sigma\gamma), \\ \kappa^+ = -\tan(\sigma\gamma) \cdot \cot((\pi/2 - \tau)\gamma), \\ 0 < \gamma < 2, \\ \max(0, \pi\gamma - \pi) < 2\gamma\tau < \min(\pi\gamma, \pi), \\ \max(0, \pi - \pi\gamma) < -2\gamma\sigma < \min(\pi, 2\pi - \pi\gamma). \end{cases}$$

The function  $v_1$  is in  $H^{1+\delta}(\Omega)$  with  $\delta < \gamma$  and thus is very singular for small parameter  $\gamma$ . For example, when  $\gamma = 0.1$ , the corresponding parameters are given by [16]

$$(5.3) \quad \kappa^+ \approx 161.4476387975881, \quad \tau = \pi/4, \quad \sigma \approx -14.92256510455152.$$

The singularity is located at the origin  $r = 0$  and polar coordinates is suitable for this problem. To avoid taking advantages from orthogonal coordinates and self-similarity of the solution, we add to the exact solution  $v_1$  a regular part

$$v_2(r, \theta) = \begin{cases} 0.08 r^2 \sin(2\theta)/\kappa^+ & \text{if } 0 \leq \theta \leq \pi/2 \text{ or } \pi \leq \theta \leq 3\pi/2, \\ 0.08 r^2 \sin(2\theta) & \text{if } \pi/2 \leq \theta \leq \pi \text{ or } 3\pi/2 \leq \theta \leq 2\pi. \end{cases}$$

and map the domain conformally to produce curved interfaces (Figure 3):

$$(5.4) \quad X + \sqrt{-1}Y = \frac{a(x + \sqrt{-1}y)}{1 + 0.02a(x + \sqrt{-1}y)}, \quad \text{where } a = \frac{1 + \sqrt{-1}}{\sqrt{2}}.$$

The exact solution is given by

$$(5.5) \quad u(X, Y) := (v_1 + v_2)(r(X, Y), \theta(X, Y)),$$

where  $r(X, Y)$  and  $\theta(X, Y)$  can be explicitly calculated from (5.4) and

$$x = r \cos \theta, \quad y = r \sin \theta.$$

In the physical domain, we also define the standard polar coordinate  $(R, \Theta)$

$$X = R \cos \Theta, \quad Y = R \sin \Theta.$$

Since the mapping (5.4) is conformal, it is easy to verify that (5.5) is also an exact solution to (1.1) and (5.1). The exact solution (5.5) is depicted in Figure 4.

The construction of a body fitting coordinate system is in general quite flexible. Here we describe a convenient way of constructing such a local coordinate system for a generic point singularity in 2D. Since the singularity is concentrated at the origin, it is therefore plausible to resolve the singularity by stretching in the radial direction. To be more precise, we denote by  $(\xi^1, \xi^2) = (\rho, \phi)$  the computational variables, with  $\rho_i = i\Delta\rho = i/N$ ,  $\phi_j = j\Delta\phi = 2\pi j/N_\phi$ ,  $0 \leq i \leq N$ ,  $0 \leq j \leq N_\phi$ . The coordinate lines  $\rho = \text{constant}$  are mapped to  $R = \text{constant}$  with the function  $R = R(\rho)$  to be specified below.

As for the  $\phi$  variable, we first map the four coordinate lines  $\phi = 0, \pi/2, \pi, 3\pi/2$  (corresponding to  $j = 0, N_\phi/4, N_\phi/2$  and  $3N_\phi/4$ ) to the four segments of  $\Gamma$ ,  $\Theta = \Theta_0(R), \Theta_1(R), \Theta_2(R)$  and  $\Theta_3(R)$  respectively. The functions  $\Theta_i(R)$  defining the

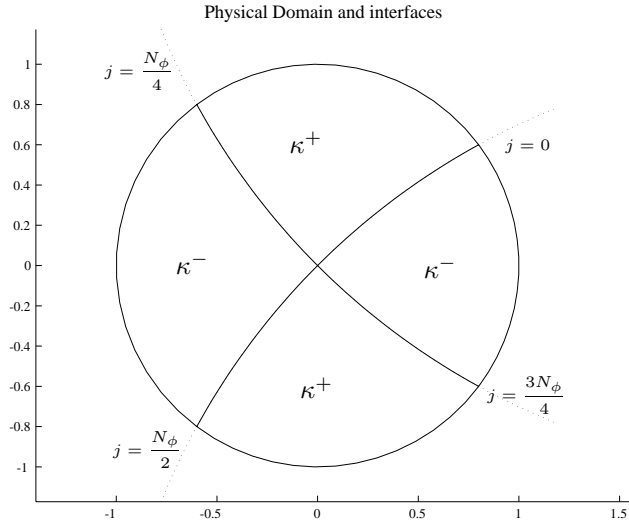


**Figure 3:** The physical domain and the curved interfaces.

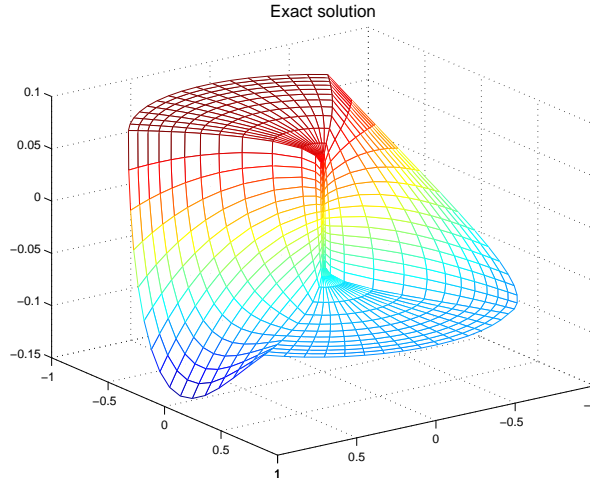


**Figure 4:** The surface plot of the exact solution.

interface  $\Gamma$  are assumed to have been explicitly given. Next we map other coordinate lines  $\phi = \text{constant}$  by equipartition in the  $\Theta$  direction. For example,

$$\Theta(\rho, \phi_j) = \Theta_0(R(\rho)) + j \left( \frac{\Theta_1(R(\rho)) - \Theta_0(R(\rho))}{N_\phi/4} \right),$$

for  $0 < j < N_\phi/4$  and so on.

In order to resolve the singularity, we start with uniform mesh  $R_i^{(0)} = \rho_i$  and iteratively compute the radial variable  $R = R^{(k)}(\rho)$  by

$$(5.6) \quad D_\rho \left( W^{(k)} D_\rho R^{(k+1)} \right) = 0, \quad \text{where } W_{i+1/2}^{(k)} = \max_j \left\{ \frac{\sqrt{h_1^2 + \left( u_{i+1,j}^{(k)} - u_{i,j}^{(k)} \right)^2}}{R_{i+1}^{(k)} - R_i^{(k)}} \right\},$$

with  $R_0^{(k)} = 0$  and  $R_N^{(k)} = 1$  held fixed.

In (5.6),  $u^{(k)}$  is the numerical solution computed from  $k$ th iterated grids and (5.6) is iterated till  $R^{(k)}$  converges. This is the classical equi-arclength distribution in the radial direction.

The final distribution of  $\{R_i\}$  is depicted in Figure 5 and 6. Note that we did not use explicit information about the order of singularity  $\gamma$  and the singularity has been well resolved automatically by this simple grid distribution strategy.

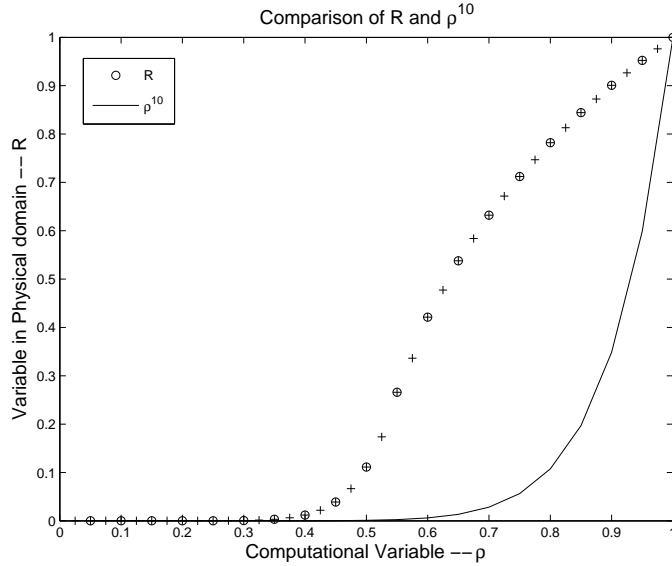


**Figure 5:** The resulted distribution of grid points  $\{R_i\}$  in the radial direction.

**Table 1:** Relative errors ( $\|u^e - u^h\|_{L^\infty} / \|u^e\|_{L^\infty}$ ) and order of accuracy in  $u^h$ .

$N \times N_\phi$	$\ u^e - u^h\ _{L^\infty} / \ u^e\ _{L^\infty}$	Order
$16 \times 48$	$3.0110E - 3$	—
$32 \times 96$	$7.3793E - 4$	2.02
$64 \times 192$	$1.8481E - 4$	2.00
$128 \times 384$	$4.6236E - 5$	2.00

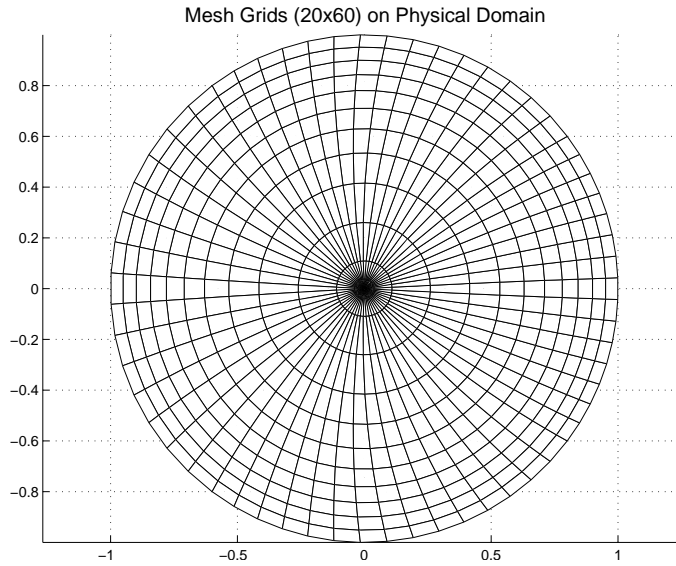


**Figure 6:** The resulted grids distribution.

**Acknowledgment:** This work is supported in part by National Science Committee of Taiwan under contracts 93-2115-M-007-011 (Wang) and 93-2811-M-007-061 (Huang).

### References

1. Ivo Babuska, *The finite element method for elliptic equations with discontinuous coefficients*, Computing (Arch. Elektron. Rechnen) **5** (1970), 207–213.
2. James H. Bramble and J. Thomas King, *A finite element method for interface problems in domains with smooth boundaries and interfaces*, Adv. Comput. Math. **6** (1996), no. 2, 109–138.
3. James H. Bramble and Vidar Thomee, *Pointwise bounds for discrete Green's functions*, SIAM J. Numer. Anal. **6** (1969), no. 4, 583–590.
4. Zhiming Chen and Shibin Dai, *On the efficiency of adaptive finite element methods for elliptic problems with discontinuous coefficients*, SIAM J. Sci. Comput. **24** (2002), no. 2, 443–462.
5. Zhiming Chen and Jun Zou, *Finite element methods and their convergence for elliptic and parabolic interface problems*, Numer. Math. **79** (1998), no. 2, 175–202.
6. Houde Han, *The numerical solutions of interface problems by infinite element method*, Numer. Math. **39** (1982), no. 1, 39–50.
7. Yin-Liang Huang, *A monotone finite difference scheme for elliptic interface problems on arbitrary domains*, Ph.D. thesis, National Tsing Hua University, Hsinchu, Taiwan, 2004.
8. R. B. Kellogg, *Singularities in interface problems*, Numerical Solution of Partial Differential Equations, II (SYNSPADE 1970) (Proc. Sympos., Univ. of Maryland, College Park, Md., 1970), Academic Press, New York, 1971, pp. 351–400.
9. R. Bruce Kellogg, *Higher order singularities for interface problems*, The Mathematical Foundations of the Finite Element Method with Applications to Partial Differential Equations (A. K. Aziz, ed.), Academic Press, New York, 1972, pp. 589–602.
10. ———, *On the Poisson equation with intersecting interfaces*, Applicable Anal. **4** (1975), 101–129.

11. O. A. Ladyzhenskaja, V. Ja. Rivkind, and N. N. Ural'ceva, *Solvability of diffraction problems in the classical sense*, Trudy Mat. Inst. Steklov. **92** (1966), 116–146 (Russian), Translated in Proceedings of the Steklov Institute of Math., no. 92 (1966), Boundary value problems of mathematical physics IV, Am. Math. Soc.
12. Randall J. LeVeque and Zhi Lin Li, *The immersed interface method for elliptic equations with discontinuous coefficients and singular sources*, SIAM J. Numer. Anal. **31** (1994), no. 4, 1019–1044.
13. Zhilin Li, Tao Lin, and Xiaohui Wu, *New Cartesian grid methods for interface problems using the finite element formulation*, Numer. Math. **96** (2003), no. 1, 61–98.
14. W. Littman, G. Stampacchia, and H. F. Weinberger, *Regular points for elliptic equations with discontinuous coefficients*, Ann. Scuola Norm. Sup. Pisa (3) **17** (1963), 43–77.
15. Xu-Dong Liu, Ronald P. Fedkiw, and Myungjoo Kang, *A boundary condition capturing method for Poisson's equation on irregular domains*, J. Comput. Phys. **160** (2000), no. 1, 151–178.
16. Pedro Morin, Ricardo H. Nochetto, and Kunibert G. Siebert, *Data oscillation and convergence of adaptive FEM*, SIAM J. Numer. Anal. **38** (2000), no. 2, 466–488 (electronic).
17. Wei-Cheng Wang, *A jump condition capturing finite difference scheme for elliptic interface problems*, SIAM J. Sci. Comput. **25** (2004), no. 5, 1479–1496.
18. Lung-An Ying, *The infinite element method*, Peking University Press, 1992 (Chinese).

DEPARTMENT OF MATHEMATICS, NATIONAL TSING HUA UNIVERSITY, HSINCHU, TAIWAN  
E-mail address: d897203@duet.am.nthu.edu.tw

DEPARTMENT OF MATHEMATICS, NATIONAL TSING HUA UNIVERSITY, HSINCHU, TAIWAN  
E-mail address: wangwc@duet.am.nthu.edu.tw